OPTOELECTRONICS AND ADVANCED MATERIALS – RAPID COMMUNICATIONS Vol. 19, Iss. 7-8, July-August 2025, p. 378 - 383

Potassium Bromide scattering simulation for improving phosphor-converting white LED performance

NGUYEN DOAN QUOC ANH[1], NGUYEN THI PHUONG LOAN[2,*], PHAM VAN DE[3], HSIAO-YI LEE[4]
[1]*Faculty of Electrical and Electronics Engineering, Ton Duc Thang University, Ho Chi Minh City, Vietnam*
[2]*Faculty of Fundamental 2, Posts and Telecommunications Institute of Technology, Ho Chi Minh City, Vietnam*
[3]*Faculty of Engineering, Dong Nai Technology University, Dong Nai Province, Vietnam*
[4]*Department of Electrical Engineering, National Kaohsiung University of Science and Technology, Kaohsiung city, Taiwan*

Potassium Bromide (KBr) is recognized for its performance in improving luminescence intensity and stability of perovskite nanocrystals for white light emitting diodes (W-LEDs). This work establishes a simulation of KBr's scattering influence of chromaticity and luminosity of the general W-LED model. The concentration of KBr varies to monitor the optical influences. The Mie-scattering and MATLAB computation are the primary simulation means. Results demonstrate the efficacy of increasing KBr amount in reducing the spatial chromatic deviation while minimizing the reduction in luminescence intensity of the W-LED. Thus, KBr owns a great potential to be a promising additive for phosphor compound for the fabrication of high-power and high-quality W-LED devices.

(Received December 23, 2024; accepted August 4, 2025)

Keywords: White LED, Lambert-Beer law, Color rendering index, Luminous efficacy

1. Introduction

White light-emitting diodes (W-LEDs) have attracted significant attention and have seen increased adoption in various applications, such as general lighting and backlight displays [1, 2]. The favorable characteristics of LEDs, including high efficiency, slim profiles, fast switching times, and low contamination, make them highly valuable for modern liquid-crystal display-based devices in comparison to conventional cold cathode fluorescent lamps [3-5]. The predominant method for achieving white light involves combining yellow light generated by the interaction of yellow phosphor $YAG:Ce^{3+}$ and silicone glue with blue light emitted from the LED chips. The yellow phosphor absorbs the blue light for the conversion of yellow light and resulting in the generation of white light with the desired color temperature. However, an imbalance between the weakening of the blue light and the strengthening of the yellow light with each absorption leads to an uneven color distribution. This disparity often manifests as the "yellow ring" around the periphery of the light on the projected surface, causing visual discomfort [6-9]. Addressing this color deviation challenge necessitates enhancing the spatial color uniformity of pc-LEDs by adjusting the range and properties of wavelengths within the phosphor. Various nanocrystals and particles, such as ZrO_2, TiO_2, $CaCO_3$, and SiO_2, have been explored to achieve color consistency. The effective use of these nanospheres for color uniformity hinges on the scattering coefficients of the phosphor-nanoparticle compound [10-13]. Typically, scattering is enhanced with the integration of these nanospheres, particularly those with high doping concentrations and small diameters. Nevertheless, the introduction of nanospheres often results in a notable decrease in luminosity due to backscattering effects [14].

Potassium Bromide (KBr) is favorable in surface modification for perovskite nanocrystals. It is reported that the potassium ions (K^+) incorporated into the perovskite nanocrystals can enhance the crystal's quantum yield and photoluminescence stability and intensity at high temperature [15]. Thus, KBr has caught significant attention from the industry as a potential addictive for enhancing white LED performance. In this paper, the simulation of the KBr's scattering and effects on white LED optical features is established. The concentration of KBr is adjusted for determining the scattering influences. Mie-scattering theory-based programs and MATLAB computation are applied to conduct the simulation and present the data [16-19]. The scattering numerical frameworks used for the simulation is demonstrated in section 2. The obtained simulation results and discussion are shown in section 3. Section 4 is the conclusion of the paper, presenting the potential of the KBr crystal and its application in future works for enriching the luminescent material resource for phosphor-converting W-LEDs [20].

2. Scattering analysis

Scattering numerical framework used for the simulation is carried out on the MATLAB program, based on the Mie theory [20-23]. The scattering processes are presented with different KBr concentrations while its particle size is constant at 5 microns. While excessively large particles sizes lead to negative effects that opposite to desirable ones resulting from smaller sizes, such as inconsistent illumination allocation, ineffective dispersion as well as illumination extrication and so on. However, if the particle size is moderately large, it can still offer several benefits in some cases. When the particle size reaches or goes beyond the wavelength for observable illumination, usually 0.4 to 0.7 μm, it can adhere to the Mie scattering principle. For this case, granules with 5 μm size may yield proficient dispersion to augment illumination extrication via phosphor sheets. Larger particle sizes also feature lower proportion between exterior zone and volume, thus lessening exterior-associated penalties and yielding greater thermic proficiency for high-power states, which proves paramount for strong-intensity LEDs that value thermic regulation. In terms of commerciality, larger particle sizes are balanced concerning both optical and production proficiency since they reduce the need for particular dispersing approaches to prevent consolidation, thus suitable for inexpensive large-scale manufacturing. The scattering coefficient $\mu_{sca}(\lambda)$ is employed for examining the scattering of KBr/phosphor compound in this paper, which can be expressed as follows:

$$\mu_{sca}(\lambda) = \int N(r) C_{sca}(\lambda, r) dr \qquad (1)$$

$$C_{sca} = \frac{2\pi}{k^2} \sum_{0}^{\infty} (2n-1)(|a_n|^2 + |b_n|^2) \qquad (2)$$

where $N(r)$ and C_{sca} indicate the particle's distribution density and the scattering cross section, respectively; λ and r signify the wavelength and particle size, respectively. For scattering cross section computation, a_n and b_n can be obtained with the following expressions:

$$a_n(x,m) = \frac{\psi_n'(mx)\psi_n(x) - m\psi_n(mx)\psi_n'(x)}{\psi_n'(mx)\xi_n(x) - m\psi_n(mx)\xi_n'(x)} \qquad (3)$$

$$b_n(x,m) = \frac{m\psi_n'(mx)\psi_n(x) - \psi_n(mx)\psi_n'(x)}{m\psi_n'(mx)\xi_n(x) - \psi_n(mx)\xi_n'(x)} \qquad (4)$$

in which $k = 2\pi/\lambda$ and $x = k.r$; m indicates the refractive index; $\psi_n(x)$ and $\xi_n(x)$ are the Riccati-Bessel functions. The scattering simulation is determined with varying KBr amount in the range of 1-21 wt%. The results and influence of scattering coefficients of the KBr in the active layer are displayed in the next section, from which the effectiveness of enhanced scattering with KBr crystals in promoting color temperature distribution uniformity can be realized [24, 25].

3. Computation and discussion

The collected scattering coefficients of KBr from 1 wt% to 21 wt% is displayed in Fig. 1. Fig. 1(a) is the scattering coefficients of 1-11 wt% KBr, and Fig. 1(b) shows that of 13-21 wt%. The KBr was reported to own high transparency under the tested light wavelengths, indicating that its light scattering could be quite low. However, owing to the impurities (mainly aluminum) in the KBr powders, the absorption was recorded. The impurities in the KBr samples contributed to higher scattering. This is due to the discrepancy among polarizability as well as latticework distance, which generates dispersion centers scattering illumination to multiple pathways. Besides, the steps of grinding the powder in the synthesis of KBr also presented effects on the scattering and absorption of the material. The scattering and absorption of the KBr can be enhanced by grinding repeatedly, especially under the short wavelengths [26]. Repeated grinding for KBr will alter its particle form as well as exterior attribute increase dispersion as well as absorption. When KBr undergoes repeated grinding, fresh crystal planes featuring unresolved bindings or defects would be constantly created. Due to KBr's attribute, these exposed planes would typically absorb background moisture, which possess their own absorption bands, leading KBr acquiring absorption attributes absent from non-exposed and unprocessed crystals. The uneven forms and coarse planes of particles resulting from extensive grinding act as a way to scatter illumination. Beside plane influences, repeated grinding will generate inner stress as well as defects inside particles. Such defects disrupt the homogeneity of the refractive index of said particles, increasing the number of dispersion centers. Such factors can be used to demonstrate the stronger scattering at short wavelength in the presence of KBr, as seen in Fig. 1.

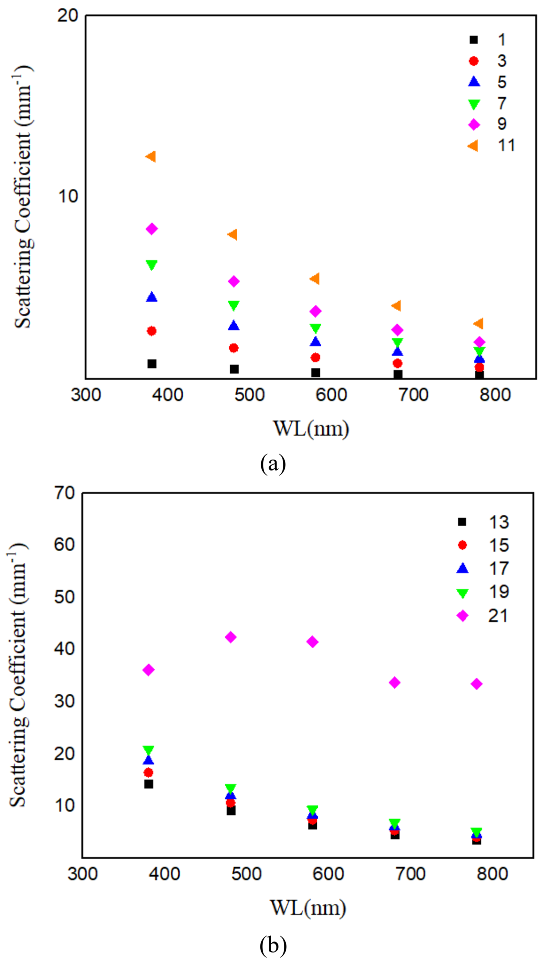

Fig. 1. Scattering coefficients of the active layer in with different KBr amounts: (a) 1-11 wt% and (b) 13-21 wt% (colour online)

As the measured wavelength is longer, the scattering coefficient decreases. The changes in the scattering coefficients is more noticeable in the KBr concentration range of 1-11 wt% (see Fig. 1(a)). The increasing concentration of KBr leads to the stronger scattering coefficient. As the concentration of KBr reaches 13-19 wt%, the increase is noted, but not too significant. When KBr amount is at 21 wt%, the scattering coefficient is the strongest and the fluctuation is different from the others under lower KBr concentration. The scattering at the blue-to-yellow region (480 – 580 nm) is the strongest, indicating that the scattering and absorption at these light wavelengths can be most effective with this KBr concentration [27].

In addition to the feature of KBr, the change in yellow phosphor concentration with increasing KBr concentration influences the scattering performance of the phosphor layer. The lower amounts of YAG:Ce^{3+} is noted with higher KBr amounts, as shown in Fig. 2. The decrease in phosphor amount in the phosphor sheet can reduce the phosphor reabsorption, leading to the greater scattering of the incident and emitted light of KBr crystals.

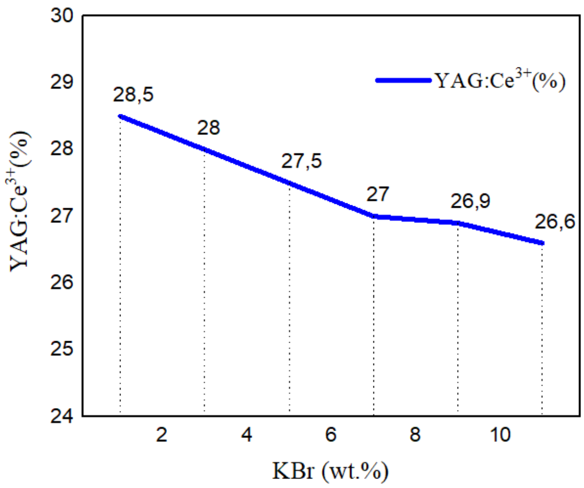

(a)

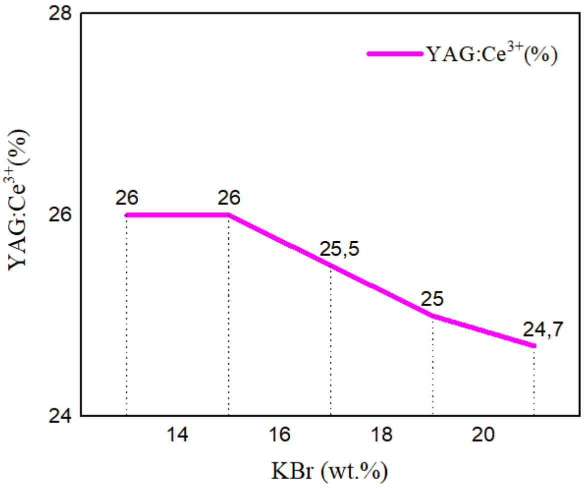

(b)

Fig. 2. Amounts of YAG:Ce^{3+} yellow phosphors (mass %) with different KBr amounts: (a) 1-11 wt% and (b) 13-21 wt% (colour online)

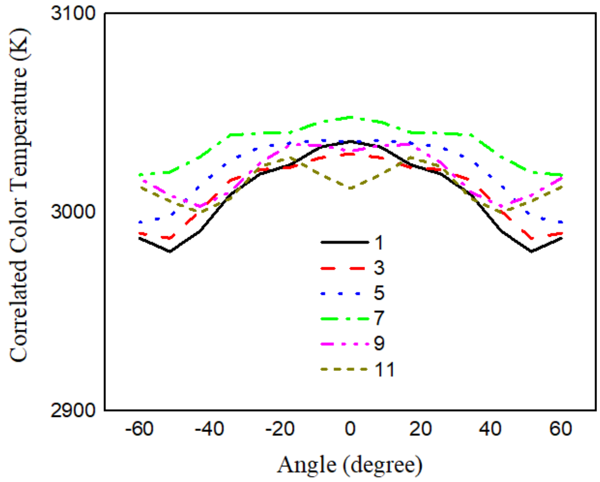

(a)

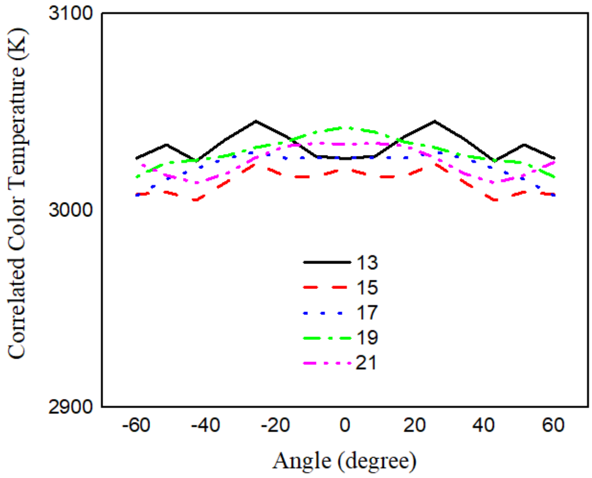

(b)

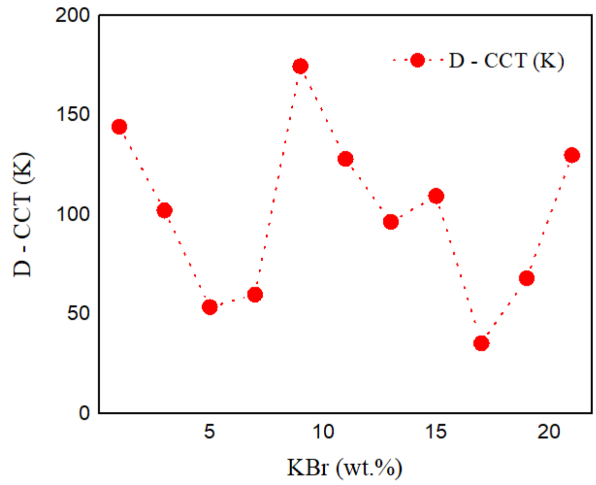

(c)

Fig. 3. The color distribution uniformity of the LED with varying KBr amounts: (a) CCT with 1-11 wt%, (b) CCT with 13-21 wt%, and (c) D-CCT levels with 1-21 wt% (colour online)

The scattering improvement can help reduce the correlated color temperature (CCT) level and enhance the uniformity of CCT distribution, which can be observed in Fig. 3. In Fig. 3(a) and (b), the CCT distribution at different angles are shown with KBr amounts of 1-11 wt% and 13-21 wt%, respectively. As seen, the increase of KBr generally reduce the light intensity at the center (0 degree) while increasing the light intensity at the larger angles. This indicates the better utilization of incident light from the LED chip (ultraviolet/near-ultraviolet/blue) for conversion and better scattering of the phosphor layer, contributing to obtain the lower color deviation. Fig. 3(c) shows the deviated CCT level (D-CCT), in which fluctuation is relatively significant. The highest D-CCT is observed with 9 wt% KBr, while the lowest CCT deviation is obtained with 17 wt% KBr. Such results demonstrate that high concentration of KBr can effectively enhance the color uniformity but increasing the KBr concentration does not always benefit the D-CCT reduction. The D-CCT variation between 9 and 17 wt.% is significant since it results in notable color disparities. Based on ellipse thresholds, the disparity can be perceived by consumers. Therefore, selecting proper KBr amount is critical to obtain the desired result [28].

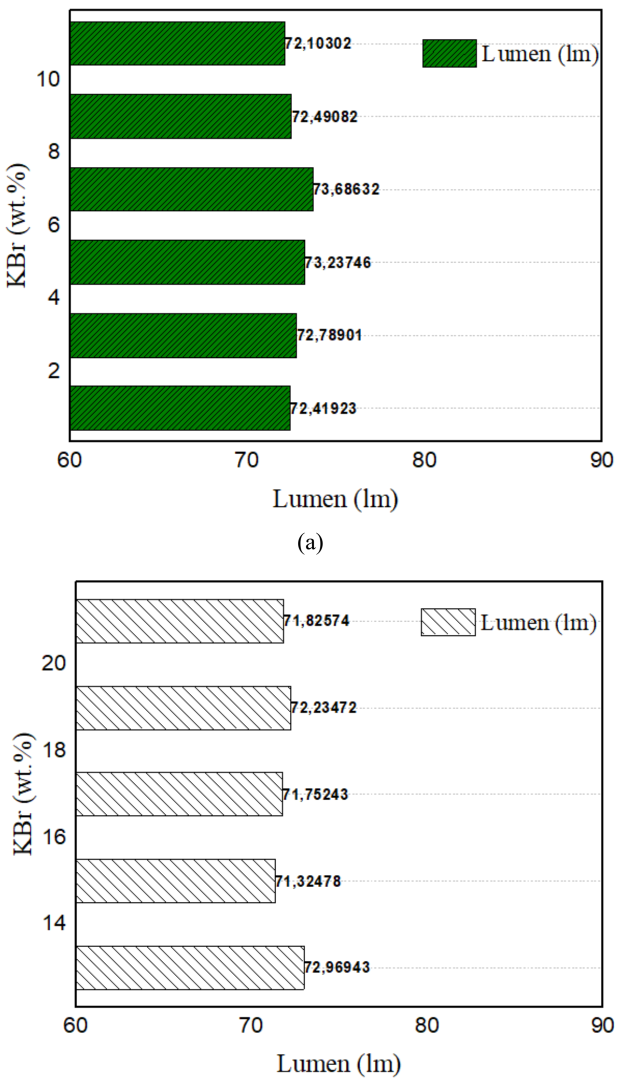

(a)

(b)

Fig. 4. Lumen with different KBr amounts: (a) 1-11 wt% and (b) 13-21 wt%

The lumen output and color rendition of the W-LED can be impacted by the increasing amount of KBr in the phosphor film. As shown in Fig. 5, the fluctuation of lumen output at different KBr concentration is insignificant. In Fig. 5 (a), the lumen starts out increasing and reaches the highest level at ~73.6 with 7 wt% KBr in the layer. As the concentration of KBr is beyond this level, the lumen decreases slightly, maintaining around 72. The lowest lumen output is recorded at ~71,3 with 15 wt% KBr, as seen in Fig. 5 (b). Shortly, the lumen output is not affected much by the increasing KBr amount.

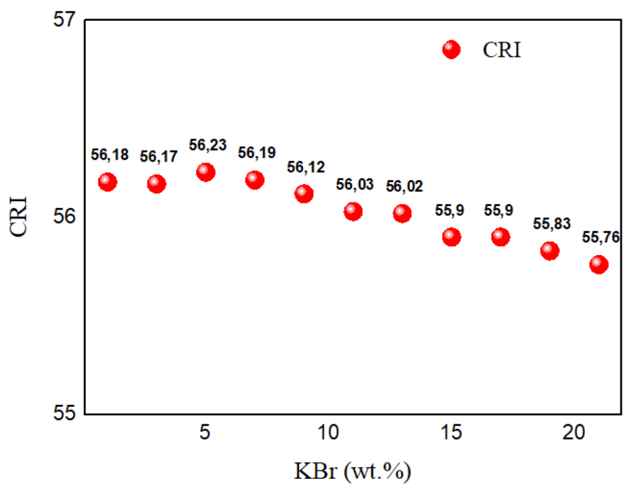

Fig. 5. CRI value with different KBr amounts

The rendition performance of the W-LED is shown in Figs. 5 and 6, where the color rendering index (CRI, Fig. 5) and color quality scale (CQS, Fig. 6) are assessed. The increasing in KBr amount leads to the decrease in both CRI and CQS. However, the reduction of CQS is relatively more significant than that of the CRI. It can be attributed to that the CQS assesses more factors for reproducing color, including the larger set of color samples, the CRI, the color coordination, and the visual preferences of the user. As a result, the reduction in CRI can induce the larger declination of the CQS.

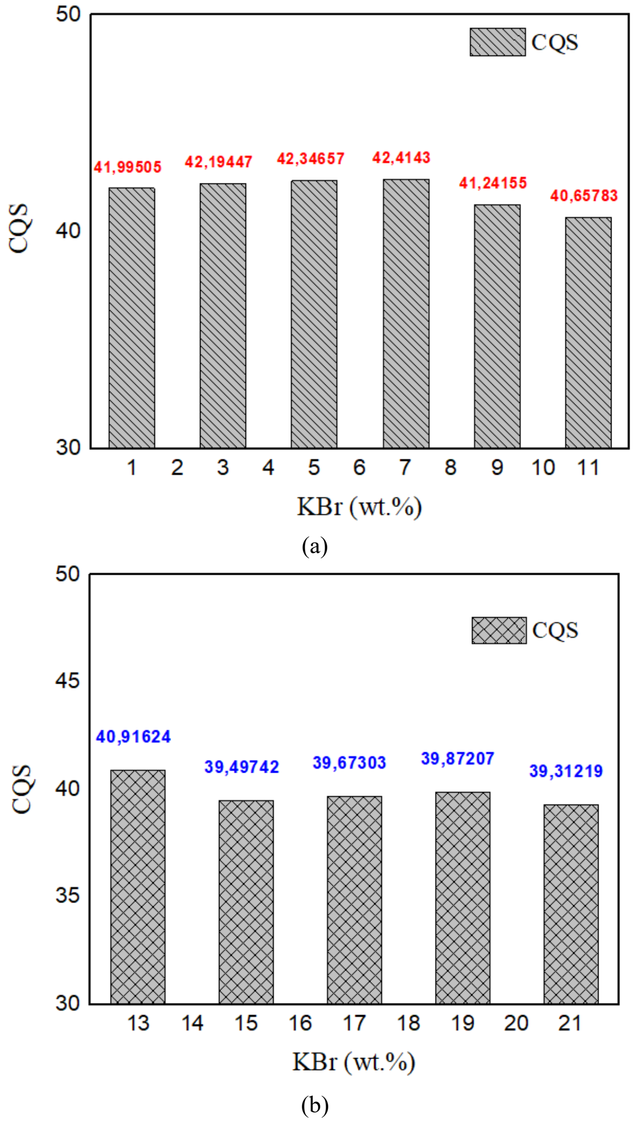

Fig. 6. CQS value with different KBr amounts: (a) 1-11 wt% and (b) 13-21 wt% (colour online)

Yet, the KBr concentration of 5-7 wt% shows the increase in both CQS and CRI. Though the increase of color rendition at this KBr's concentration range is not critically noticeable, the D-CCT does show significant reduction (see Fig. 3) and the lumen is also increase and reaches the highest value (see Fig. 4). Such results indicate that 5-7 wt% KBr should be opted for the overall improvement of W-LED light performance.

4. Conclusions

The paper involved conducting a simulation to investigate the impact of KBr scattering on the chromaticity and luminosity of a typical W-LED model. Mie-scattering theory and MATLAB computation were employed as the primary simulation methods to observe the optical effects resulting from varying KBr concentrations. The findings revealed that higher concentrations of KBr led to an increased scattering coefficient, effectively improving color uniformity. However, the relationship between higher KBr concentrations and the reduction of D-CCT was not consistently evident. While CRI and CQS show fluctuations when KBr increased, these fluctuations were restricted to a particularly small range. Nonetheless, an increase in these parameters was observed with 5-7 wt% KBr. Hence, the careful selection of the appropriate KBr concentration was underscored as crucial in achieving the desired outcomes.

Acknowledgment

The author wishes to express their gratitude to the Posts and Telecommunications Institute of Technology, Vietnam, for financial support for this research.

References

[1] G. Cao, W. Li, S. Huang, J. He, Electr. Pow. Compo. Sys. **47**, 515 (2019).
[2] M. Y. Mehr, A. Bahrami, W. D. van Driel, X. J. Fan, J. L. Davis, G. Q. Zhang, Int. Mater. Rev. **65**, 102 (2020).
[3] M. Hämmer, A. Gassmann, A. Reller, H. V. Seggern, O. Gutfleisch, R. Stauber, J. Zimmermann, Mater. Technol. **34**, 178 (2019).
[4] X. Wang, M. Sun, Y. Fu, W. Liu, Q. Wang, C. Wang, J. Li, J. Asian Ceram. Soc. **9**, 782 (2021).
[5] P. W. Nolte, N. Ziegeler, A. C. Rimbach, S. Schweizer, Quant. Infrared Thermogr. J. **17**, 96 (2020).
[6] H. T. Tung, N. D. Q. Anh, H. Y. Lee, Optoelectron. Adv. Mat. **18**(1-2), 58 (2024).
[7] H. E. Dillon, C. Ross, R. Dzombak, LEUKOS **16**, 229 (2020).
[8] B. Zhao, Q. Xu, M. R. Luo, J. Opt. Soc. Am. A **37**, 1257 (2020).
[9] Q. Xu, B. Zhao, G. Cui, M. R. Luo, Opt. Express **29**, 7778 (2021).
[10] M. Safdar, P. Emmel, J. Opt. Soc. Am. A **38**, 140 (2021).
[11] X. Kong, M. J. Murdoch, I. Vogels, D. Sekulovski, I. Heynderickx, J. Opt. Soc. Am. A **36**, 1022 (2019).
[12] R. A. Deshpande, A. S. Roberts, S. I. Bozhevolnyi, Opt. Mater. Express **9**, 717 (2019).
[13] S. K. Abeysekera, V. Kalavally, M. Ooi, Y. C. Kuang, Opt. Express **28**, 130 (2020).
[14] S. S. Panda, H. S. Vyas, R. S. Hegde, Opt. Mater. Express **10**, 3145 (2020).
[15] X. Kong, M. Wei, M. J. Murdoch, I. Vogels, I. Heynderickx, J. Opt. Soc. Am. A **37**, 521 (2020).
[16] Q. Xu, L. Meng, X. Wang, Appl. Opt. **58**, 7649 (2019).
[17] C. Wu, Z. Liu, Z. Yu, X. Peng, Z. Liu, X. Liu, X. Yao, Y. Zhang, Opt. Express **28**, 19085 (2020).
[18] M. Vanoli, M. Grassi, F. Lovati, S. Barzaghi, T. MP

Cattaneo, A. Rizzolo, J. Near Infrared Spectrosc. **27**, 54 (2019).
[19] P. Liu, Z. Guan, T. Zhou, Q. Xie, Q. Yu, Y. He, Z. Zeng, X. Wang, Appl. Opt. **60**, 5652 (2021).
[20] C. Shin, H. Wu, K. Kwon, Y. Piao, K. Lee, S. Gil, N. Kim, Opt. Express **29**, 1175 (2021).
[21] W. Bao, M. Wei, K. Xiao, J. Opt. Soc. Am. A **37**, 671 (2020).
[22] V. O. Yachnaya, V. R. Lutsiv, J. Opt. Technol. **88**, 647(2021).
[23] H. Jiang, Z. Lin, Y. Li, Y. Yan, Z. Zhou, E. Chen, Q. Yan, T. Guo, Appl. Opt. **60**, 6971 (2021).
[24] H. T. Tung, N. D. Q. Anh, H. Y. Lee, Optoelectron. Adv. Mat. **18**, 1–2, 58 (2024).
[25] N. D. Q. Anh, H. V. Ngoc, Materials Science-Poland **38**, 493 (2020).
[26] M. H. N. Thi, P. T. That, N. D. Q. Anh, Materials Science-Poland **38**, 594 (2020).
[27] N. T. P. Loan, N. D. Q. Anh, Optoelectron. Adv. Mat. **15**(1-2), 71 (2021).
[28] P. T. That, N. T. P. Loan, L. V. Tho, N. D. Q. Anh, H. -Y. Liao, G. F. Luo, H. Y. Lee, Materials Science-Poland **38**, 667 (2020).

*Corresponding author: ntploan@ptithcm.edu.vn